

Spectroscopy of photonic bands in macroporous silicon photonic crystals

M. Galli, M. Agio, L. C. Andreani, M. Belotti, G. Guizzetti, F. Marabelli, and M. Patrini
INFN - Dipartimento di Fisica "A. Volta," Università di Pavia, Via Bassi 6, I-27100 Pavia, Italy

P. Bettotti, L. Dal Negro, Z. Gaburro, and L. Pavesi
INFN-Dipartimento di Fisica, Università di Trento, Via Sommarive 14, I-35040 Povo, Italy

A. Lui and P. Bellutti
Istituto di Ricerca Scientifica e Tecnologica, IRST-ITC, Via Sommarive, I-35040 Povo, Italy
 (Received 6 December 2001; published 8 March 2002)

Variable-angle reflectance performed on macroporous silicon photonic crystals yields the dispersion of two-dimensional photonic bands. A comparison with calculated optical spectra identifies the spectral structures, which mark the onset of a propagating photonic mode, as one-dimensional critical points. The experimental results agree with theoretical determinations of the reflectance and of the photonic-band dispersion in a wide energy range. A symmetry analysis yields the selection rules for excitation of photonic modes, which can be treated like elementary excitations of the crystal.

DOI: 10.1103/PhysRevB.65.113111

PACS number(s): 42.70.Qs, 78.20.Ci, 78.67.Bf, 81.07.Bc

Photonic crystals are new materials where the propagation properties of photons are dramatically changed because of the periodic variation of the dielectric function. They are attracting great interest in view of achieving, e.g., control of spontaneous emission,¹ localization of light,² or propagation in bent waveguides.³ The periodicity of the refractive index leads to the validity of Bloch theorem and to the concept of *photonic bands*. These are, however, not easy to measure. Photonic bands have first been determined in the microwave regime by phase-sensitive transmission measurements⁴ that yield the wave vector inside the crystal at a given frequency. In-plane transmission in two-dimensional (2D) waveguide photonic crystals has been used to map the photonic bands from Fabry-Pérot fringes within the sample.⁵ Another technique for measuring 2D photonic bands in a waveguide⁶ relies on the observation of sharp structures in reflectance from the surface, which arise from coupling of the incoming radiation field to guided modes of the structure due to the patterning. Since the wave vector \mathbf{k}_{\parallel} parallel to the waveguide plane is conserved, each resonant structure in reflectance yields a point of the $\omega(\mathbf{k}_{\parallel})$ dispersion in a given direction of the Brillouin zone.

In this paper we show that *photonic bands can be measured by variable-angle reflectance even if no waveguide is present*: the technique is used here to obtain the photonic-band dispersion in a plane parallel to the surface. This opens new possibilities to measure the photonic dispersion even in 3D photonic crystals. We perform reflectance measurements from the surface of macroporous silicon samples patterned with a triangular lattice of holes. Unlike waveguide-based photonic crystals, macroporous silicon can be considered as homogeneous along the pore axis (taken as z), since pores of 50–100 μm depth can be achieved.⁷ The refractive index is modulated only in the xy plane, however, the 2D photonic bands retain an out-of-plane dispersion. Thus the spectral structures in reflectance used for the determination of the bands mark the *onset* of a diffracted beam. *The process for the excitation of a photonic mode is shown to be similar to*

the absorption threshold in insulating solids and results in a spectral line shape analogous to that of critical-point features in semiconductors.^{8,9}

Spectroscopic studies of electronic and vibrational excitations in solids often rely on *selection rules*. Here we perform a symmetry analysis of the photonic bands and of the reflectance experiment. At normal incidence, where the Γ point of the 2D Brillouin zone is probed, the symmetry of the point group drastically limits the number of observable modes. At oblique incidence along the main symmetry directions of the lattice, we show that mirror symmetry with respect to the plane of incidence (rather than the xy plane of the 2D crystal) must be used for classifying “allowed” and “forbidden” bands.

Macroporous samples were prepared by the already well-described method of electrochemical etch of a prepatterned substrate.⁷ Briefly, triangular and square patterns were defined by lithography and the initial etch pits were transferred to the substrate by a hot KOH treatment. The successive electrochemical etching allows to make deeper pores while maintaining their cross section. Substrates of various resistivities were used, here we focused on an n -type sample with 8–12 $\Omega\text{ cm}$ resistivity. As the substrate was n -type doped, light assistance was used and provided by a tungsten lamp, which was stabilized in current. Here we present results on a sample¹⁰ with triangular structure and lattice constant $a = 2\ \mu\text{m}$. The sample was polished with diamond powder to eliminate the etch pits. The holes have a nearly circular shape with radius $r = 0.24a$ (air fraction ~ 0.21); atomic force microscopy (AFM) image of the sample is shown in the inset of Fig. 2.

In Fig. 1 we show the photonic bands of the 2D structure for in-plane propagation, calculated with standard plane-wave expansion.^{3,11,12} Due to mirror symmetry with respect to the xy plane the bands separate into E modes (fields components E_z, H_x, H_y) and H modes (components H_z, E_x, E_y).¹³ The symmetry classification of photonic bands is also indicated. The point group of the triangular lattice is

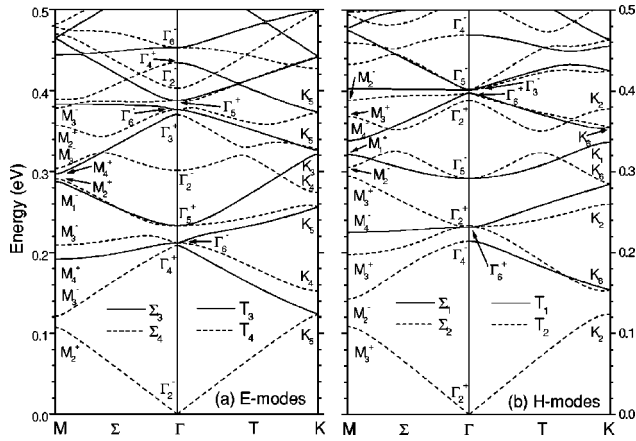


FIG. 1. Photonic bands of the triangular lattice of air holes in Si with $a=2 \mu\text{m}$, $r/a=0.24$: (a) E modes, (b) H modes.

D_{6h} , which is useful to view as the direct product of C_{6v} and C_s ,¹⁴ where C_s contains the identity and the specular reflection σ_{xy} . The small point groups at the main symmetry points are D_{2h} at M and D_{3h} at K . The small point group is C_{2v} for the Γ - M , Γ - K , and M - K directions, however, the twofold axis of C_{2v} differs in the three cases. Note that the twofold degenerate levels at Γ can have Γ_5^+ or Γ_6^- symmetries for E modes and Γ_5^- , Γ_6^+ for H modes; Γ_5^- (Γ_5^+) is the symmetry of the xy components of a pseudovector (vector).

Variable-angle specular reflectance from the sample surface was measured in the spectral range 0.15–0.5 eV with a Fourier-transform spectrometer (Bruker IFS66/S) at a spectral resolution of 1 meV. The angle of incidence θ is defined with an angular resolution of $\pm 1^\circ$. A liquid-nitrogen-cooled InSb photodiode was used as a detector and a silver mirror was used as a reference. Measurements were done along the Γ - K and Γ - M orientations both in transverse electric (TE) and transverse magnetic (TM) polarization by means of a polypropylene wire-grid polarizer. We also calculate reflectance at different angles of incidence by the scattering matrix method,¹⁵ which can be applied to any patterned multilayer structure: in the present case we only have two semi-infinite layers, namely, air and patterned silicon. We remark that the method is an exact solution of Maxwell equations and includes all diffraction processes in Si as well as in air.

In Fig. 2 we show the reflectance of the sample for TE-polarized light incident along the Γ - M orientation; in Fig. 3 we show a comparison of measured and calculated¹² reflectance along Γ - K for TE and TM polarizations. The reflectance curves of the macroporous silicon sample display prominent features with a well-defined dispersion as a function of incidence angle. There is a good overall agreement between experimental and calculated spectra for the number of the structures and their angular dispersion, although the experimental line shape is in some cases more complex than the theoretical one. The spectral strength of the structures depends markedly on the angle θ . Most features become vanishingly weak at $\theta=5^\circ$, where only one strong structure at 0.29 eV is observed.

The results of Figs. 2 and 3 (and the analogous ones for TM-polarized light along Γ - M , not shown) are interpreted in

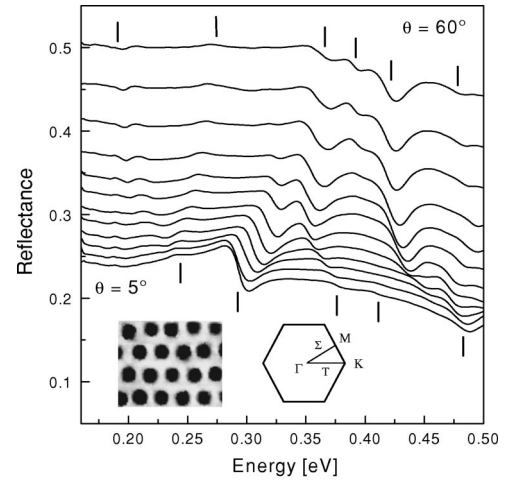


FIG. 2. Reflectance of the macroporous silicon sample for TE-polarized light incident along the Γ - M orientation. The angle of incidence θ is varied from 5° to 60° with a step of 5° . The curves at 5° , 10° , and 15° are slightly offset for clarity. Vertical bars mark the positions of 2D photonic modes for 5° and 60° . Insets: AFM micrograph of the sample (dimensions: $10 \times 8.4 \mu\text{m}$) and 2D Brillouin zone.

the following way. When the frequency ω and the parallel wave vector \mathbf{q}_{\parallel} of the incoming beam [of modulus $q_{\parallel} = (\omega/c)\sin\theta$] match those of a photonic mode propagating in the plane, a diffracted beam is created in the material and a corresponding structure appears in reflectance. This is very clear in the calculation, where the onset of a diffracted beam

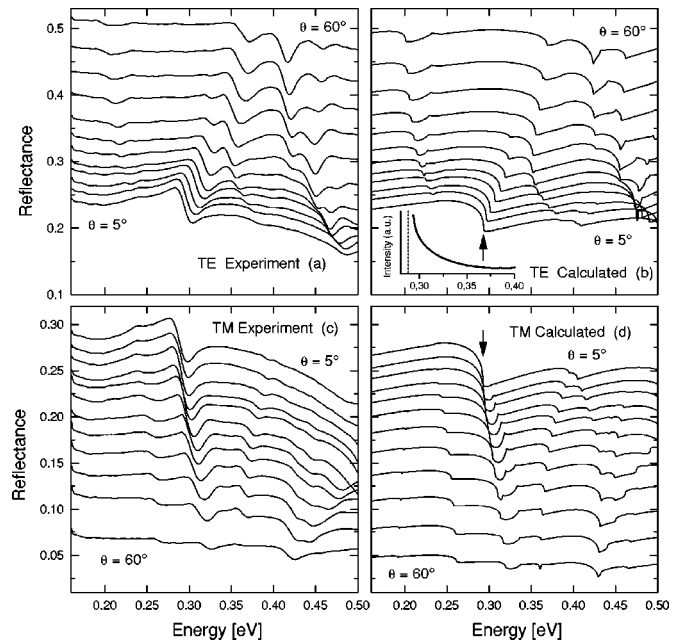


FIG. 3. (a),(c) experimental reflectance of the sample for light incident along the Γ - K orientation, for TE and TM polarizations; (b),(d) calculated reflectance. The angle of incidence θ is varied from 5° to 60° with a step of 5° . The curves at 5° , 10° , and 15° are slightly offset for clarity. Inset to (b): diffracted intensity corresponding to the allowed mode at $\theta=5^\circ$ (onset marked by arrows).

corresponds to a complex wave-vector component k_z that goes through zero and becomes real. In Ref. 6 a similar approach was used for patterned $\text{Al}_x\text{Ga}_{1-x}\text{As}$ waveguides. However, in the present case, there is no waveguide and a structure in reflectance marks the *onset* of a photonic mode, which is excited and remains propagating also for higher frequencies.¹⁶ Since most structure in reflectance spectra show a typical dispersive shape we took the inflection point as energy position for each propagating mode (see marks in Fig. 2). In this way the uncertainty in determining energy bands is estimated to be ± 5 meV.

At each structure in the calculated reflectance spectrum the derivative is discontinuous, such as for critical-point transitions.^{8,9} This “universal” line shape is broadened in the experiments, probably because of sample inhomogeneity. Each critical point in reflectance is related to a singularity in the diffracted intensity $D(\omega)$, which may be calculated by interpreting the excitation of a photonic mode as an “absorption” process (the intensity of the diffracted beam is removed from specular reflectance and transmittance): thus $D(\omega)$ may be expressed as

$$D(\omega) \propto \int d\mathbf{k}_{\parallel} \int dk_z \delta_{\mathbf{k}_{\parallel}, \mathbf{q}_{\parallel}} \delta(\hbar\omega - E(\mathbf{k}_{\parallel}, k_z)),$$

where $q_{\parallel} = (\omega/c)\sin\theta$. The parallel wave vector $\mathbf{k}_{\parallel} \equiv \mathbf{q}_{\parallel}$ is conserved and the out-of-plane dispersion of all bands (except close to the special point $\omega=0$) is quadratic in k_z around $k_z=0$,³ with a threshold $E(\mathbf{k}_{\parallel}, 0) \equiv E_0$. Thus we get $D(\omega) \propto (\hbar\omega - E_0)^{-1/2}$, like for a 1D density of states. The inset of Fig. 3(b) shows the calculated diffracted intensity of the allowed mode at near-normal incidence, which indeed has the form of an inverse square root close to the threshold $E_0 = 0.29$ eV. A similar behavior is found for all diffracted rays. Thus we conclude that each spectral feature in reflectance corresponds to a 1D critical point.

We now discuss the selection rules for specular reflectance. The surface of the crystal breaks mirror symmetry with respect to the xy plane: thus the reflection σ_{xy} is not a symmetry operation anymore. The photonic modes should then be classified according to the subgroup C_{6v} of the point group at Γ and the corresponding subgroups at other k points. Along the Γ - M and Γ - K directions the small point group becomes C_s , i.e., specular reflection with respect to the plane of incidence is the only symmetry operation besides the identity.

The general selection rule can be stated as follows: *a photonic band can appear in reflectance only if it has the same symmetry of the incident electromagnetic field.* At normal incidence, the electric field (E_x, E_y) as well as the magnetic field (H_x, H_y) transform similar to the twofold degenerate representation Γ_5^- of C_{6v} . The irreducible representations of D_{6h} that reduce to this representation are Γ_5^+ and Γ_5^- : thus only states with symmetries Γ_5^{\pm} can appear in reflectance. This selection rule is obeyed in reflectivity curves of Figs. 2 and 3: in particular, the strong structure around 0.29 eV at $\theta=5^\circ$ corresponds to the allowed band with symmetry Γ_5^- [H modes in Fig. 1(b)].

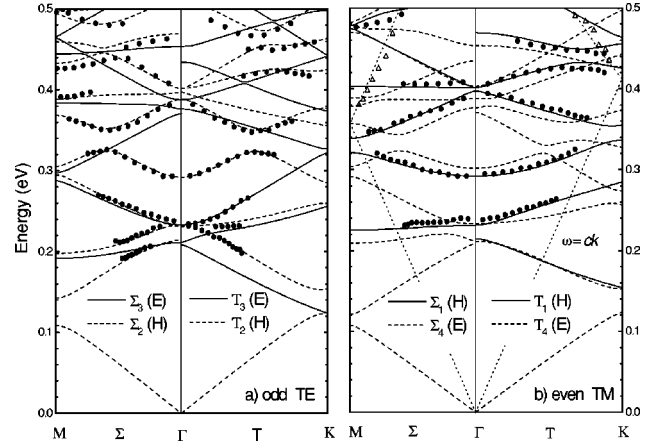


FIG. 4. Points: measured dispersion of the photonic bands, derived from the structures in reflectance curves; solid and dashed lines: photonic bands of the triangular lattice of air holes, separated according to parity with respect to the plane of incidence: (a) TE polarization, odd modes, (b) TM polarization, even modes. The open triangles in (b) represent diffraction in air and must be compared with the folded dispersion of free photons (dotted lines).

Concerning now selection rules along Γ - M and Γ - K , we notice that these are the only orientations for which the plane of incidence is also a mirror plane of the structure: thus the photonic bands can be classified as even or odd with respect to this mirror symmetry. Now, a TE wave is odd for specular reflection with respect to the plane of incidence, while a TM wave is even. Thus a TE-polarized wave interacts with photonic bands that are *odd* for specular reflection in the vertical mirror plane, while a TM-polarized wave interacts only with *even* bands. Odd photonic bands correspond to Σ_3 and Σ_2 representations of C_{2v} for Γ - M (T_3 and T_2 for Γ - K), while even bands correspond to Σ_1 and Σ_4 for Γ - M (T_1 and T_4 for Γ - K).

Notice that an incident plane wave can interact with both E and H modes of the photonic structure. It is, therefore, appropriate to compare the photonic bands extracted from a reflectivity experiment not with those of E and H modes, but rather with those of the same parity with respect to specular reflection in the plane of incidence. Such a comparison is shown in Fig. 4. It can be seen that some nondegenerate bands “stop” at the Γ point for a given polarization and “restart” in the other polarization: this peculiar behavior is due to the fact that the mirror plane changes when turning from the Γ - M to the Γ - K direction. The experimental points agree very well with the calculated photonic bands of the proper parity. Anticrossings are seen to occur between bands of the same symmetry, e.g., between two Σ_2 states and between two T_2 states around 0.3–0.36 eV.

Not all bands that are allowed by symmetry appear in reflectance curves. This is not in contrast with the selection rule: an allowed band may have a nonzero, yet very weak spectral strength. Indeed, theoretical simulations with a very fine mesh indicate that weaker structures are present, which in the experiments fall below the signal-to-noise ratio. It is interesting to remark that most measured photonic bands correspond to H modes. This may be understood since at normal

incidence the Γ_5^- mode at 0.29 eV is much more intense than Γ_5^+ . At oblique incidence, the photonic bands that are forbidden at $\mathbf{k}_\parallel=0$ gain spectral strength by mixing with allowed bands; since only one strong feature Γ_5^- is present below 0.5 eV, most photonic bands that appear in reflectance in this energy range have H mode character.

The experimental points marked by open triangles in Fig. 4(b) have a steep dispersion and do not match any photonic band of the Si material. They, however, match the dispersion of light in air, folded in the first Brillouin zone: the corresponding structures in reflectance mark the onset of diffraction in air. These structures depend only on the Bravais lattice (not on the pore shape or depth) and would be present also for a shallow grating.¹⁷ In the present context, these “Wood anomalies” represent photonic bands in the upper half-space and are intermixed with photonic bands of the Si crystal.

The 2D photonic bands of macroporous silicon photonic

crystals have been determined by variable-angle reflectance: the spectral features, which yield the energy position of a photonic mode at $k_z=0$, are interpreted as 1D critical points. The same technique applied to three-dimensional modulated systems would yield the photonic-mode dispersion in a plane parallel to the surface. Only bands with the same symmetry of the incident electromagnetic field can appear in reflectance. The selection rules derived from symmetry have a form similar to those for direct excitation of phonons or excitons. The present results show that the photonic modes behave similar to other elementary excitations in solids. This suggests new interesting research possibilities where spectroscopic studies of material excitations radiatively coupled to photonic modes can be envisaged.

The authors are grateful to D. Wiersma for useful suggestions. This work was supported by MURST through the PRIN 2000 project “One- and two-dimensional photonic crystals: growth, theory, and optical properties.”

¹E. Yablonovitch, Phys. Rev. Lett. **58**, 2059 (1987).

²S. John, Phys. Rev. Lett. **58**, 2486 (1987).

³J. D. Joannopoulos, R. D. Meade, and J. N. Winn, *Photonic Crystals* (Princeton University Press, Princeton, NJ, 1995).

⁴E. Yablonovitch and T. J. Gmitter, Phys. Rev. Lett. **63**, 1950 (1989); W. M. Robertson *et al.*, J. Opt. Soc. Am. B **10**, 322 (1993).

⁵D. Labilloy *et al.*, Phys. Rev. B **59**, 1649 (1999); H. Benisty *et al.*, J. Lightwave Technol. **17**, 2063 (1999).

⁶V. N. Astratov *et al.*, Phys. Rev. B **60**, 16 255 (1999).

⁷U. Grüning, V. Lehmann, S. Ottow, and K. Busch, Appl. Phys. Lett. **68**, 747 (1996); A. Birner, R. B. Wehrspohn, U. Gösele, and K. Busch, Adv. Mater. **13**, 377 (2001).

⁸F. Bassani and G. Pastori Parravicini, *Electronic States and Optical Transitions in Solids* (Pergamon, Oxford, 1975).

⁹P. Y. Yu and M. Cardona, *Fundamentals of Semiconductors* (Springer-Verlag, Berlin, 1996).

¹⁰The etching parameters were: HF solution 2.5M in H₂O/EtOH = 1/1 (vol); photocurrent density $J=10$ mA/cm² with +4V bias; etching time 2400 s.

¹¹K. M. Ho, C. T. Chan, and C. M. Soukoulis, Phys. Rev. Lett. **65**,

3152 (1990).

¹²We use 151 plane waves for both the photonic bands and the reflectance calculation. For the photonic bands we assume $\epsilon=11.8$ for Si, while for the reflectance we take into account the (small) frequency dispersion of ϵ .

¹³We purposely avoid calling these modes TM and TE, as often done: we reserve this terminology to mirror symmetry with respect to the plane of incidence in the interpretation of reflectivity experiments.

¹⁴We use notations of G. F. Koster, J. O. Dimmock, R. G. Wheeler, and H. Statz, *Properties of the Thirty-Two Point Groups* (MIT Press, Cambridge MA, 1963).

¹⁵D. M. Whittaker and I. S. Culshaw, Phys. Rev. B **60**, 2610 (1999).

¹⁶The variable-angle reflectance technique as applied here is different from experiments performed on 3D systems like inverse opals, see, e.g., M. S. Thijssen *et al.*, Phys. Rev. Lett. **83**, 2730 (1999): in that case the Bragg peak in reflectance yields information on the photonic gap and on its angular dispersion, but not on the band dispersion parallel to the surface as done here.

¹⁷R. W. Wood, Philos. Mag. **4**, 396 (1902).